Platelet concentrate-derived extracellular vesicles promote adult hippocampal neurogenesis

Ariunjargal NyamErdene[1], Nhi Thao Ngoc Le[1], Ouada Nebie[2], Emilie Faivre[2,3], Liling Delila [4], Ming-Li Chou[4], Joshua R Lowe[5], Kadiombo Bantubungi[6], Luc Buée[2,3], Tara L Walker[5], David Blum[2,3,4*], Thierry Burnouf[1,4, 7,8*]

[1]International Ph.D. Program in Biomedical Engineering, College of Biomedical Engineering, Taipei Medical University, Taipei ,Taiwan, [2]University of Lille, Inserm, CHU Lille, UMR-S1172 Lille Neuroscience & Cognition (LilNCog), Lille, France, [3]Alzheimer and Tauopathies, LabEx DISTALZ, France, [4]Graduate Institute of Biomedical Materials and Tissue Engineering, Taipei Medical University , Taipei, Taiwan, [5]Clem Jones Centre for Ageing Dementia Research, Queensland Brain Institute, The University of Queensland, Brisbane, Australia, [6] Inserm UMR-1011, University of Lille, Lille, France, [7]International Ph.D. Program in Cell Therapy and Regeneration Medicine, [8]Ph.D. Program in Graduate Institute of Mind Brain and Consciousness, College of Humanities and Social Sciences, Taipei Medical University , Taipei , Taiwan.

Correspondence: thierry@tmu.edu.tw, david.blum@inserm.fr

Keywords: Platelet extracellular vesicles, platelet lysates, neurogenesis, regenerative medicine, intranasal delivery, brain repair.

Abstract word count: 164/200
Word Count: 1494/1500
Figures: 3
Supplementary figures: 5
Supplementary tables: 3
References: 25

Abstract

Emerging evidence suggests that platelet concentrate (PC) derivatives harbor neuroregenerative potential. Here, we evaluated the neurogenic effects of PC-derived human platelet lysate (HPPL) and extracellular vesicles (pEVs) on neural precursor cells using both an *ex vivo* neurosphere assay and an *in vivo* intranasal delivery model in adult mice. pEVs selectively enhanced the proliferation of dentate gyrus (DG)-derived neurospheres, and this region-specific effect persisted even without exogenous growth factors. In line with these findings, short-term intranasal administration of pEVs significantly increased cell proliferation in the DG. Long-term (28-day) pEVs treatment further elevated the proportion of newborn mature neurons in the DG, whereas HPPL primarily increased both proliferation and the number of immature neurons. Proteomic profiling of DG tissue after pEV treatment revealed 111 differentially expressed proteins, enriched in pathways related to oxidative phosphorylation, myelination, Notch4 signaling, and MHC class I processing. These findings identify allogeneic PC-derived EVs as potent, cell-free agents capable of promoting adult hippocampal neurogenesis and brain repair through metabolic and immunoregulatory mechanisms.

KEY POINTS

- Platelet concentrate-derived extracellular vesicles (pEVs) enhance proliferation of adult neural progenitors in the dentate gyrus (DG), and activate myelination and immune metabolic pathways linked to neuronal integration.
- pEVs represent a minimally invasive, neuroregenerative biotherapy for brain repair.

Introduction (218 words)

Adult neurogenesis, the generation of new neurons in the mature brain, persists throughout life and contributes to brain plasticity.[1,2] It occurs primarily in the subventricular zone (SVZ), supporting olfaction, and in the subgranular zone (SGZ) of the hippocampal dentate gyrus (DG), linked to learning and cognition.[3,4] Although hippocampal neurogenesis declines with age, it can be restored by interventions such as exercise,[5] partly mediated by exerkines including platelet factor 4 (PF4).[6] Enhancing endogenous neurogenesis holds promise for treating age-related and neurodegenerative disorders.

Beyond their hemostatic role,[7] platelets contribute to tissue repair, angiogenesis and neuroprotection.[8] They store and release neurotransmitters and a broad range of trophic factors from their dense and alpha granules,[9,10] which may modulate neural progenitor proliferation and support adult neurogenesis.

Platelet lysates have shown beneficial effects in animal models of stroke,[11] traumatic brain injury [8,12] and various neurodegeneration diseases[13-16] but their impacts on adult neurogenesis remain unclear. Platelet extracellular vesicles (pEVs)[17,18] carry bioactive cargo with potential to modulate neurogenic processes.[19] Hippocampal neurogenesis play a crucial role in learning and memory processes, which are particularly vulnerable in neurodegenerative conditions. Thus, we investigated the effects of pEVs isolated from platelet concentrate supernatants and a known neuroprotective, heat-treated human platelet pellet lysate (HPPL, control)[12,13] on adult hippocampal neurogenesis, using ex vivo neurosphere assays and in vivo intranasal delivery in mice.

Study design (213 words):

The experimental design is shown in Figures 1A–B, 2A, and 3A. Detailed protocols are provided in the Supplemental Data.

Animals and ethics: Eight-week-old female C57BL/6J mice were housed under standard conditions. All procedures were approved by the ULille and TMU Ethics Committees.

Neural precursor cell culture: Dentate gyrus (DG) tissue from adult mice was isolated and cultured in Neurobasal medium supplemented with B-27, GlutaMAX, antibiotics, and with or without EGF and FGF-2 (20 ng/mL each). Cultures were treated with 0.5% pEVs, 0.5% HPPL, or left untreated. Neurospheres were counted and measured at day 10.

In vivo neurogenesis: Mice received 30 µL of intranasal pEVs, HPPL, or PBS control, either daily for three days or 3 times/week for 28 days. EdU (50 mg/kg) was administered intraperitoneally (six injections over three days). Mice were perfused with saline followed by 4% PFA. Brains were post-fixed, cryoprotected, sectioned coronally or sagittally, and sections were analyzed in matched DG regions.

Label-free proteomics: HPPL and pEVs used for treatment and DG tissue harvested 28 days post-initial treatment were extracted and analyzed by LC-MS/MS. The complete proteomics datasets are provided as Supplemental Files.

Statistical analysis: One-way ANOVA with Dunnett's post hoc test was used (GraphPad Prism v10.2.3). $p < 0.05$ was considered significant. Replicates are indicated in figure legends.

Results and Discussion (1063words)

We first used an *in vitro* neurosphere assay to compare the effects of the platelet-derived preparations, pEVs and HPPL, on neural precursor cell proliferation. We found that pEVs selectively increased the size but not the number of the DG-derived neurospheres, suggesting enhanced proliferative capacity (Figure 1A and 1C). These region-specific responses persisted without the addition of EGF and FGF-2 (Supplementary Figure 1A). To address cellular uptake, both platelet preparations were labeled with Alexa Fluor 488 and applied to neurospheres for 24

hours. Fluorescence microscopy confirmed internalization of both (Supplementary Figure 1B), supporting their bioactivity *in vitro*.

We next evaluated *in vivo* neural precursor proliferation using a short-term (3-day) intranasal delivery protocol with concurrent EdU injections to label the dividing cells (Figure 1B). This revealed that pEVs significantly increased the number of proliferating EdU^+ cells in the dentate gyrus (DG) compared to PBS and HPPL treatments (Figure 1D-E). To assess long-term DG neurogenesis, a separate cohort of mice received intranasal pEVs or HPPL 3times/week for 28 days. EdU injections were administered during the first three days to label dividing cells (Figure 2A). At day 28, neuronal fate was evaluated by co-staining EdU with either DCX and NeuN, markers of immature and mature neurons, respectively. HPPL treatment increased the total number of EdU^+ cells in the DG, indicating enhanced cellular proliferation/survival (Figure 2B-C). When analyzing the phenotype of these EdU^+ cells, HPPL significantly elevated the proportion of EdU^+/DCX^+ immature neurons (Figure 2B-C). In contrast, pEVs showed a trend toward increased EdU^+ cell numbers, though this effect did not reach statistical significance (Figure 2B-D). Importantly, pEVs treatment significantly elevated the proportion of $EdU^+/NeuN^+$ mature neurons in the DG granule cell layer (Figure 2B-D).

To unveil the mechanisms underlying the effects of pEVs on hippocampal neurogenesis, we performed a proteomic analysis of DG tissue following 28 days of intranasal pEV or PBS treatment (N = 2 per group; Figure 3A). 2,656 proteins were identified in the pEV group versus 2,629 in the PBS group, with 2,580 proteins (95.4%) shared. 76 proteins were unique to pEV-treated tissue, and 49 to PBS (Figure 3B). GO-term analysis of the 76 pEV-specific proteins in DG tissue showed enrichment in protein binding and cell adhesion molecule binding functions (Supplementary Table 1; Supplementary Figure 2). Differential proteomic analysis identified 111 significantly regulated proteins, with 61 upregulated and 50 downregulated (Figure 3C). The upregulated proteins were primarily associated with biological processess of CNS myelination, oxygen binding, and postsynaptic signaling, and were enriched in oxidative phosphorylation and neuroplasticity-related KEEG pathways (Figure 3D, red). Among the most significantly upregulated proteins were those linked to neurogenesis, including angiotensin-converting enzyme (ACE; Log_2FC: 1.6537), which suggests altered regulation of the renin-angiotensin system. Structural neuronal proteins were also

elevated, such as internexin neuronal intermediate filament protein Alpha (INA; Log_2FC: 1.0899) and developmentally regulated GTP-binding Protein 1 (DRG1; Log2FC: 1.2182). Additionally, proteins associated with neuronal maturation, including Ras-related protein Rab-7a (RAB7; Log_2FC: 0.917) and brain abundant membrane-attached signal protein 1 (BASP1; Log_2FC: 0.7989) were upregulated (Figure 3D). In contrast, downregulated proteins were predominantly enriched in biological processes related to cytoplasmic translation, actin filament organization, and cell migration (Figure 3D, blue). They included key cytoskeletal regulators such as Rho-associated coiled-coil containing protein kinase 1 (ROCK1; Log2FC: -0.7107), known for its role in actin dynamics and cell proliferation[20], as well as stathmin 1 (STMN1), a regulator of microtubule stability, and Ras-related C3 botulinum toxin substrate 1 (RAC1), a GTPase involved in lamellipodia formation. The reduced expression of these proteins suggests diminished migratory activity as neurons settle into their final positions. Protein-protein interaction (PPI) analysis supported the identified biological processes, with upregulated proteins clustering in myelination and proteasome pathways, and downregulated proteins linked to translation. Full network details can be found in (Supplementary Figure 3-4). Ingenuity Pathway Analysis (IPA) confirmed activation of respiratory electron transport, myelination, and ubiquitination pathways (Figure 3E). IPA also uniquely identified activation of Notch4 signaling, critical for neural stem cell maintenance[21] and MHC class I antigen presentation, suggesting coordinated neurogenic and immune-related responses following pEV treatment.

To explore potential mechanisms by which pEVs influence adult neurogenesis, we characterized their physical and molecular properties. Cryo-EM confirmed the vesicular nature of pEVs, showing typical double-membrane structures (Supplementary Figure 5B). Particle size and concentration, measured by dynamic light scattering and nanoparticle tracking analysis, indicated a mean diameter of ~165 nm and a high particle yield (~10^{12} particles/mL) (Supplementary Figure 5C-D). SDS-PAGE revealed distinct protein profiles between pEVs and HPPL (Supplementary Figure 5E), highlighting their compositional differences. Exo-Check analysis confirmed the presence of classical EV markers (CD63, TSG101, CD81), platelet-specific CD41, and EV-associated CD9 (Supplementary Figure 5F-G). In addition, pEVs contained a subset of proteins potentially involved in neural regulatory processes.

LC-MS/MS analysis of the pEVs themselves revealed a proteome distinct from that of HPPL. Among the identified proteins, 313 were shared between the two preparations, while 63 were unique to pEVs and 582 to HPPL (Supplementary Figure 5H). Notably, ~12% of the pEV-specific proteins were complement-related proteins (Supplementary Figure 5I, 5J). This finding is consistent with the enrichment of MHC class I antigen presentation pathways identified by IPA, suggesting a functional link between the pEV proteome and the neuroimmune responses observed *in vivo*. Complement components are increasingly recognized not only for their immune functions but also for their role in neurodevelopmental processes, including synaptic pruning[22], neuroinflammation[23] and regulation of the stem cell niche[24]. Additionally, ~1% of the pEV proteome consisted of extracellular matrix (ECM) and cell adhesion molecules (Supplementary Figure 5I), including CD44, LYVE1, and HABP2 (Supplementary Table3). These proteins interact with hyaluronan, a key ECM component regulating neural stem cell maintenance and proliferation[25].

Considering the bioactive cargo enriched within pEVs and their impact on DG tissue proteomics, our findings reveal a distinct molecular signature, consistent with neurogenic activity. The upregulation of neuronal structural proteins (INA, DRG1) and maturation-associated factors (RAB7, BASP1) alongside the downregulation of cytoskeletal regulators (ROCK1, STMN1, RAC1) and axonal growth markers (GAP43), indicates a shift from neural progenitor proliferation to differentiation and circuit integration. This neurogenic transition is further supported by the activation of pathways involved in respiratory electron transport, myelination, and Notch4 signaling, while the downregulation of ribosomal quality control mechanisms and RNA decay suggests metabolic reprogramming during neuronal maturation. Collectively, these molecular changes position pEVs as potent inducers of adult neurogenesis in the dentate gyrus and open new avenues for the clinical application of platelet concentrate derivatives.

Acknowledgments

We thank the Taipei Blood Center (Guangdu, Taiwan) for supplying the platelet concentrates and the Consortia of Key Technologies and Instrumentation Center at National Taiwan University for providing mass spectrometry technical services for brain tissue analysis. This research was

supported by grants from the National Science and Technology Council (NSTC 113-2923-E-038-001), the National Health Research Institutes (NHRI-EX114-11431NI), Taiwan, and the WILL Chair France 2023 to TB, and the NSTC 114 -2927-I-038 -504 -/Inserm grant to DB and TB. AN was supported by a 2-years PhD fellowship from Taipei Medical University, TB lab funding, and a MobLilex travel grant from ULille.

Authorship

Author contributions: AN performed the experiments, analyzed the data and drafted the manuscript. LNTN conducted the proteomics analysis. ON performed part of the intranasal administrations at Lille University. EF assisted with the analysis of the brain sections. LD assisted with intranasal administration and mouse sacrifice procedures at TMU. MC assisted in proteomics data interpretation and design of figures. JL performed parallel ex vivo neurosphere assays using platelet lysates and discussed data. KB suggested and provided recommendations for the ex vivo neurosphere assays. LB contributed to methodological recommendations and funding. TLW provided expert recommendations all along the study, conducted data analysis, and drafted the manuscript. DB and TB are PhD co-advisors of AN, conceived the study design, provided funding support, and drafted the manuscript. All authors revised and approved the final version.

Conflict-of-interest disclosure: There is no conflict of interest.

ORCID profile: AN, 0000-0002-2901-0486; NTNL, 0000-0002-9540-8564; ON, 0000-0002-6802-4215; EF, 0000-0002-8608-9848; LD, 0000-0003-4979-3489; MC, 0000-0002-6996-5332; JL, 0000-0001-8981-8332; KB, 0000-0002-6152-5623; LB, 0000-0002-6261-4230; TW, 0000-0002-8472-0245; DB, 0000-0001-5691-431X; TB, 0000-0002-0507-9243

Correspondence: Thierry Burnouf, Graduate Institute of Biomedical Materials and Tissue Engineering, College of Biomedical Engineering, Taipei Medical University Shuang-Ho campus, No. 301, Yuantong Rd., Zhonghe Dist., New Taipei City 235, Taiwan. Email: thierry@tmu.edu.tw; thburnouf@gmail.com

REFERENCES

1. Kase Y, Shimazaki T, Okano H. Current understanding of adult neurogenesis in the mammalian brain: how does adult neurogenesis decrease with age? *Inflammation and Regeneration*. 2020;40(1):10.
2. Schoenfeld TJ, Cameron HA. Adult Neurogenesis and Mental Illness. *Neuropsychopharmacology*. 2015;40(1):113-128.
3. Jurkowski MP, Bettio L, K. Woo E, Patten A, Yau S-Y, Gil-Mohapel J. Beyond the Hippocampus and the SVZ: Adult Neurogenesis Throughout the Brain. *Frontiers in Cellular Neuroscience*. 2020;Volume 14 - 2020.
4. Ghosh HS. Adult Neurogenesis and the Promise of Adult Neural Stem Cells. *J Exp Neurosci*. 2019;13:1179069519856876.
5. Ávila-Gámiz F, Pérez-Cano AM, Pérez-Berlanga JM, et al. Sequential treadmill exercise and cognitive training synergistically increase adult hippocampal neurogenesis in mice. *Physiology & Behavior*. 2023;266:114184.
6. Leiter O, Brici D, Fletcher SJ, et al. Platelet-derived exerkine CXCL4/platelet factor 4 rejuvenates hippocampal neurogenesis and restores cognitive function in aged mice. *Nat Commun*. 2023;14(1):4375.
7. Smyth SS, McEver RP, Weyrich AS, et al. Platelet functions beyond hemostasis. *Journal of Thrombosis and Haemostasis*. 2009;7(11):1759-1766.
8. Nebie O, Carvalho K, Barro L, et al. Human platelet lysate biotherapy for traumatic brain injury: preclinical assessment. *Brain*. 2021;144:3142-3158.
9. Li D, Huang L-T, Zhang C-p, Li Q, Wang J-H. Insights Into the Role of Platelet-Derived Growth Factors: Implications for Parkinson's Disease Pathogenesis and Treatment. *Frontiers in Aging Neuroscience*. 2022;Volume 14 - 2022.
10. Duerschmied D, Mammadova-Bach E, Mauler M, Braun A. Immuno-Thrombotic Effects of Platelet Serotonin. In: Fatima-Shad K, ed. Serotonin - A Chemical Messenger Between All Types of Living Cells. Rijeka: IntechOpen; 2017.
11. Hayon Y, Dashevsky O, Shai E, Varon D, Leker RR. Platelet lysates stimulate angiogenesis, neurogenesis and neuroprotection after stroke. *Thrombosis and Haemostasis*. 2013;110(2):323-330.
12. Delila L, Nebie O, Le NTN, et al. Neuroprotective effects of intranasal extracellular vesicles from human platelet concentrates supernatants in traumatic brain injury and Parkinson's disease models. *Journal of Biomedical Science*. 2024;31(1):87.
13. Chou ML, Wu JW, Gouel F, et al. Tailor-made purified human platelet lysate concentrated in neurotrophins for treatment of Parkinson's disease. *Biomaterials*. 2017;142:77-89.
14. Gouel F, Timmerman K, Gosset P, et al. Whole and fractionated human platelet lysate biomaterials-based biotherapy induces strong neuroprotection in experimental models of amyotrophic lateral sclerosis. *Biomaterials*. 2022;280.
15. Anitua E, Pascual C, Pérez-Gonzalez R, Orive G, Carro E. Intranasal PRGF-Endoret enhances neuronal survival and attenuates NF-κB-dependent inflammation process in a mouse model of Parkinson's disease. *Journal of Controlled Release*. 2015;203:170-180.
16. Anitua E, Pascual C, Antequera D, et al. Plasma rich in growth factors (PRGF-Endoret) reduces neuropathologic hallmarks and improves cognitive functions in an Alzheimer's disease mouse model. *Neurobiology of Aging*. 2014;35(7):1582-1595.

17. Welsh JA, Goberdhan DC, O'Driscoll L, Théry C, Witwer KW. MISEV2023: An updated guide to EV research and applications. *Journal of Extracellular Vesicles*. 2024;13(2):e12416.
18. Burnouf T, Chou ML, Lundy DJ, Chuang EY, Tseng CL, Goubran H. Expanding applications of allogeneic platelets, platelet lysates, and platelet extracellular vesicles in cell therapy, regenerative medicine, and targeted drug delivery. *J Biomed Sci*. 2023;30(1):79.
19. Carney RP, Mizenko RR, Bozkurt BT, et al. Harnessing extracellular vesicle heterogeneity for diagnostic and therapeutic applications. *Nature Nanotechnology*. 2025;20(1):14-25.
20. Chong C-M, Ai N, Ming-Yuen Lee S. ROCK in CNS: different roles of isoforms and therapeutic target for neurodegenerative disorders. *Current drug targets*. 2017;18(4):455-462.
21. Hollville E, Romero SE, Deshmukh M. Apoptotic cell death regulation in neurons. *Febs j*. 2019;286(17):3276-3298.
22. Stevens B, Johnson MB. The complement cascade repurposed in the brain. *Nature Reviews Immunology*. 2021;21(10):624-625.
23. Bohlson SS, Tenner AJ. Complement in the Brain: Contributions to Neuroprotection, Neuronal Plasticity, and Neuroinflammation. *Annual Review of Immunology*. 2023;41(Volume 41, 2023):431-452.
24. Fatoba O, Itokazu T, Yamashita T. Complement cascade functions during brain development and neurodegeneration. *The FEBS Journal*. 2022;289(8):2085-2109.
25. Wilson E, Knudson W, Newell-Litwa K. Hyaluronan regulates synapse formation and function in developing neural networks. *Scientific Reports*. 2020;10(1):16459.

Legends

Figure 1. pEVs and HPPL Differentially Regulate Neural Precursor Cell Proliferation *Ex Vivo* and *In Vivo* at Day 3. (A) Schematic representation of neural stem cell isolation from the dentate gyrus (DG) followed by neurosphere generation. **(B)** Schematic representation of the short-term (3-day) intranasal delivery protocol for pEVs or HPPL, combined with EdU (50 mg/kg) i.p administration twice daily at 6-hour intervals. **(C)** Quantification of neurosphere number and size distribution from DG-derived cultures following treatment with platelet concentrate-derived extracellular vesicles (pEVs) or heat-treated platelet pellet lysate (HPPL). The size of 50 neurospheres was analyzed per condition. For neurosphere number, all visible neurospheres were counted in 80 wells of a 96-well plates per condition. Data are mean ± SEM from five independent experiments. ***$p < 0.001$ vs PBS using one-way ANOVA followed by Dunnett's multiple comparisons post-hoc test. Control condition is normalized to 100%, and that pEVs and HPPL values represent the relative change in neurosphere size and number compared to this baseline. **(D)** Quantification of total EdU^+ cells across 5 DG sections/animal along the granular layer in DG. Data are mean ± SEM (N = 18 animals per group). *$p < 0.05$ vs PBS using one-way ANOVA followed by Dunnett's multiple comparisons post-hoc test. **(E)** Representative confocal images of EdU^+ cells in the DG following 3-day treatment with pEVs or HPPL. Green channel represents EdU-labeled cells, and blue channel shows DAPI nuclear staining. Images acquired by Stellaris confocal microscopy with (20× objectives). Scale bar: 100 µm (inset: 50 µm). These data highlight that pEVs exert a preferential impact on DG as compared to HPPL.

Figure 2. pEVs promote neurogenesis in the dentate gyrus (DG) of hippocampus. **(A)** Experimental design schematic showing long-term (28-day) intranasal administration protocol for pEVs and HPPL combined with EdU (50 mg/kg) labeling regimen (twice daily at 6-hour intervals). **(B)** Quantification shows total EdU^+ cells across 5 DG sections/animal along the granular layer in DG, percentage of co-expressing DCX^+/EdU^+ and $NeuN^+/EdU^+$ cells in the granular layer of DG region. Data represent mean ± SEM (N = 18 animals per group). Statistical significance determined by ordinary one-way ANOVA followed by Dunnett's (*$p < 0.05$, **$p < 0.01$ ***$p < 0.001$) *with multiple comparisons post-hoc test.* **(C-D)** Representative images of immature/mature neurons co-expressing DCX^+/EdU^+ and $NeuN^+/EdU^+$ in the granular layer of DG following pEVs & HPPL treatment at day 28. DCX is illustrated by gray channel, EdU by green channel, and NeuN, by red channel. Scale bars: 50 µm; inset scale bar: 20 µm. White arrows indicate DCX^+/EdU^+, and $NeuN^+/EdU^+$ co-expressing cells, orange arrows indicate DCX^-/EdU^+, and $NeuN^-/EdU^+$ cells. Representative images were captured using Stellaris confocal microscopy with (63× objectives). Data indicate that pEVs significantly increase the proportion of $NeuN^+$ cells among EdU^+ cells in the DG, suggesting enhanced neuronal differentiation, while HPPL primarily promotes cell proliferation and increases the number of immature neurons in the DG.

Figure 3. Proteomic profiling reveals pEVs-induced molecular changes in the dentate gyrus (DG) of hippocampus. (A) Experimental workflow showing DG tissue collection following 28-day of intranasal administration of pEVs or PBS as control, followed by proteomic profiling via LC-MS/MS. **(B)** Venn diagram illustrating the overlap of identified proteins in DG tissue from pEVs and PBS-treated groups, highlighting both shared and treatment-specific proteins. **(C)** The differentially expressed proteins (DEPs) were identified by comparing proteins commonly

expressed between pEV-treated samples and PBS controls. Volcano plot analysis of these DEPs in DG tissue following pEV treatment revealed significant changes using thresholds of $p \leq 0.05$ and fold change ≥ 1.2. Red and blue points on the plot indicate significantly upregulated and downregulated proteins, respectively. **(D)** Gene Ontology (GO) enrichment of upregulated and downregulated DEPs categorized by biological process, molecular function, and cellular component. Neurogenesis Pathway Proteins Altered by EV Treatment: Upregulated and Downregulated Proteins with Log2FC Values, KEGG pathway analysis is shown for both subsets. **(E)** Canonical pathway analysis of differentially expressed proteins (DEPs) using Ingenuity Pathway Analysis (IPA), highlighting significantly altered signaling networks ($p < 0.05$) after DG_EV treatment compared to PBS. Pathways are color-coded by activation z-score: orange bars indicate predicted activation (positive z-score), blue bars indicate predicted inhibition (negative z-score), and white bars indicate pathways with z-score = 0. The green line represents the ratio of DEPs present in each pathway relative to the total proteins in that pathway.

Figure 1

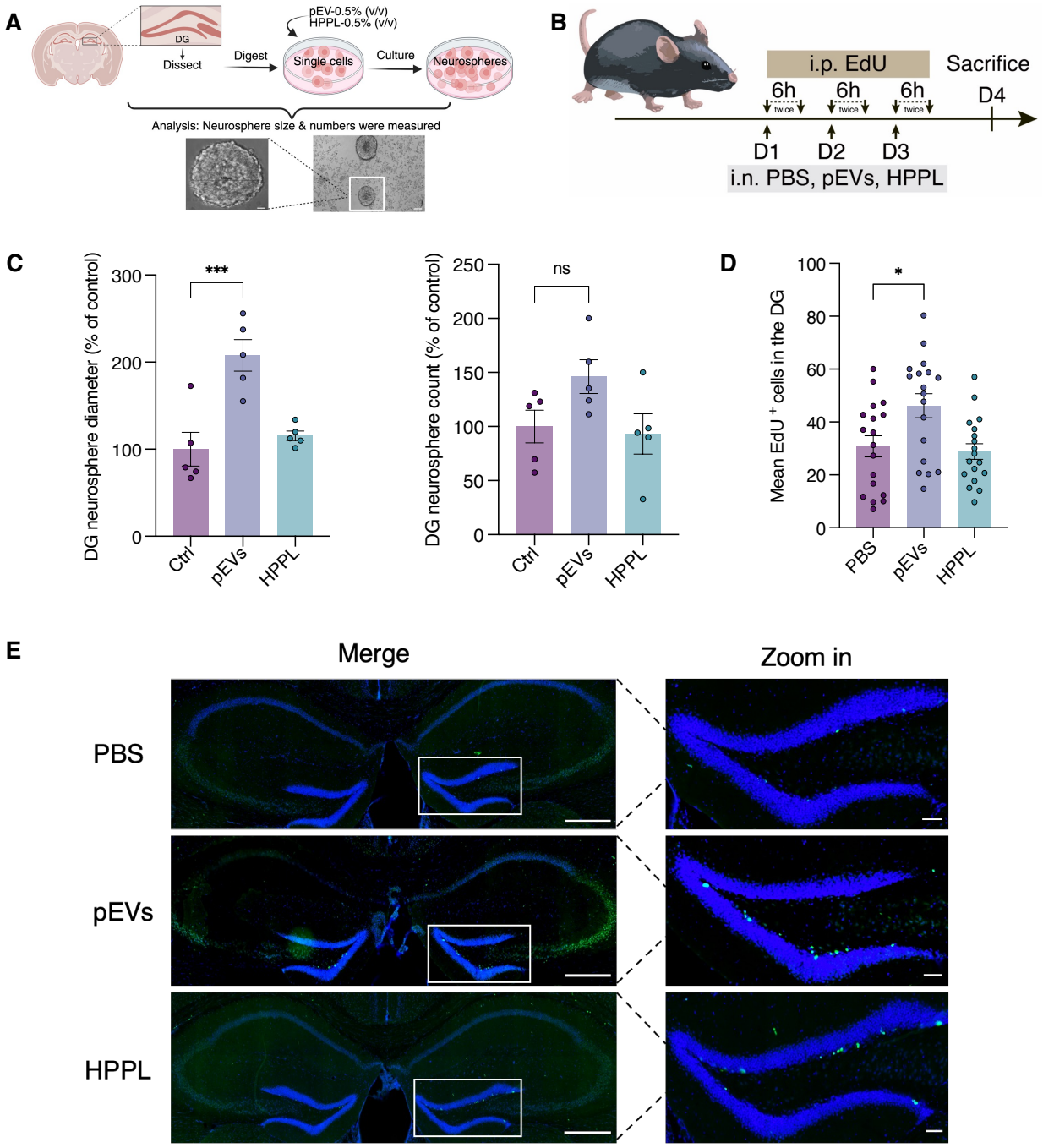
A
DG
Dissect
Digest
pEV-0.5% (v/v)
HPPL-0.5% (v/v)
Single cells
Culture
Neurospheres
Analysis: Neurosphere size & numbers were measured
B
i.p. EdU
Sacrifice
6h
twice
D4
D1
D2
D3
i.n. PBS, pEVs, HPPL
C
DG neurosphere diameter (% of control)
***
Ctrl
pEVs
HPPL
DG neurosphere count (% of control)
ns
D
Mean EdU+ cells in the DG
*
PBS
E
Merge
Zoom in
PBS
pEVs
HPPL

Figure 2

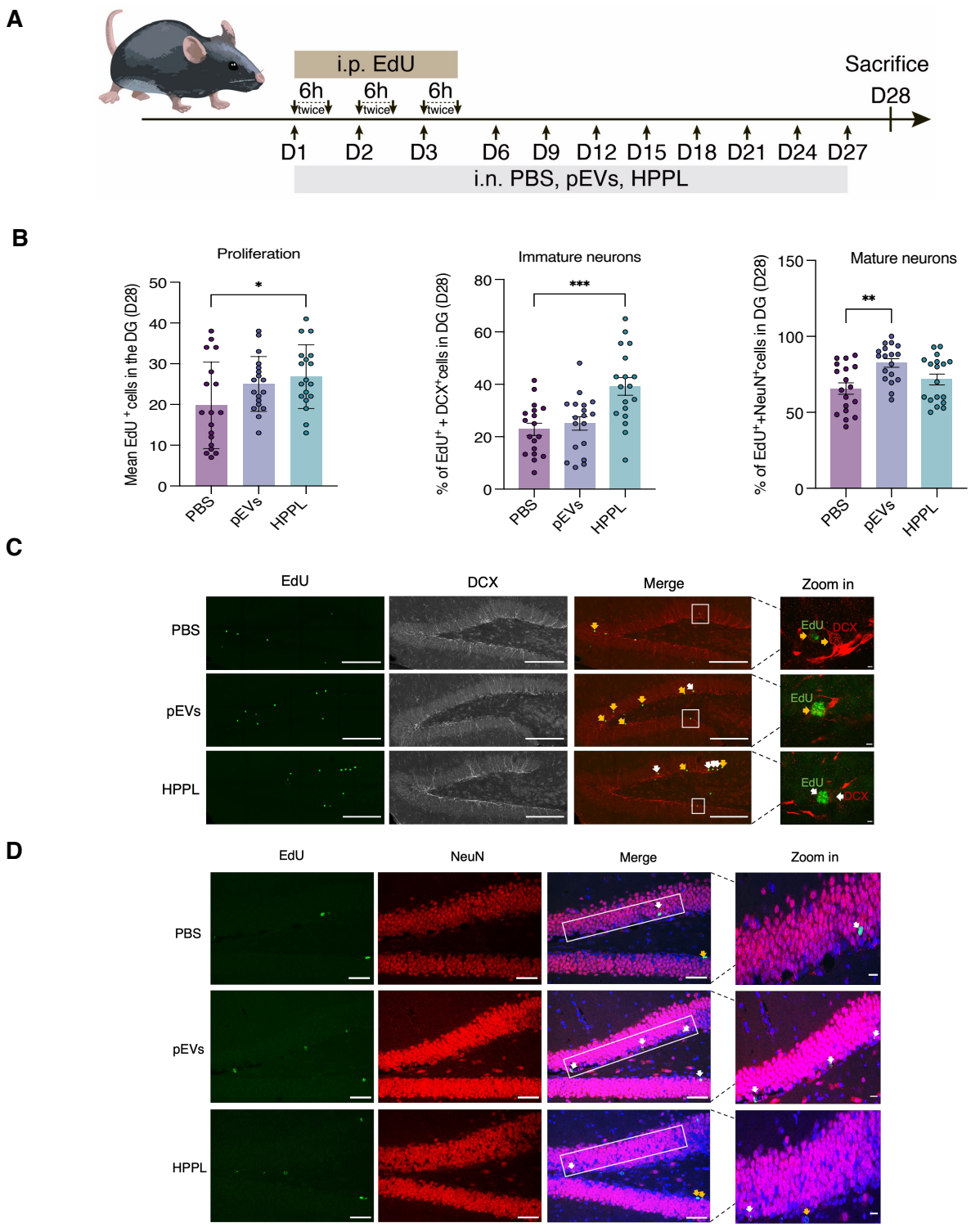
A
i.p. EdU
6h
twice
6h
twice
6h
twice
Sacrifice
D28
D1
D2
D3
D6
D9
D12
D15
D18
D21
D24
D27
i.n. PBS, pEVs, HPPL
B
Proliferation
Mean EdU + cells in the DG (D28)
Immature neurons
% of EdU+ + DCX+cells in DG (D28)
Mature neurons
% of EdU+ +NeuN+cells in DG (D28)
PBS
pEVs
HPPL
C
EdU
DCX
Merge
Zoom in
PBS
pEVs
HPPL
D
EdU
NeuN
Merge
Zoom in
PBS
pEVs
HPPL

Figure 3

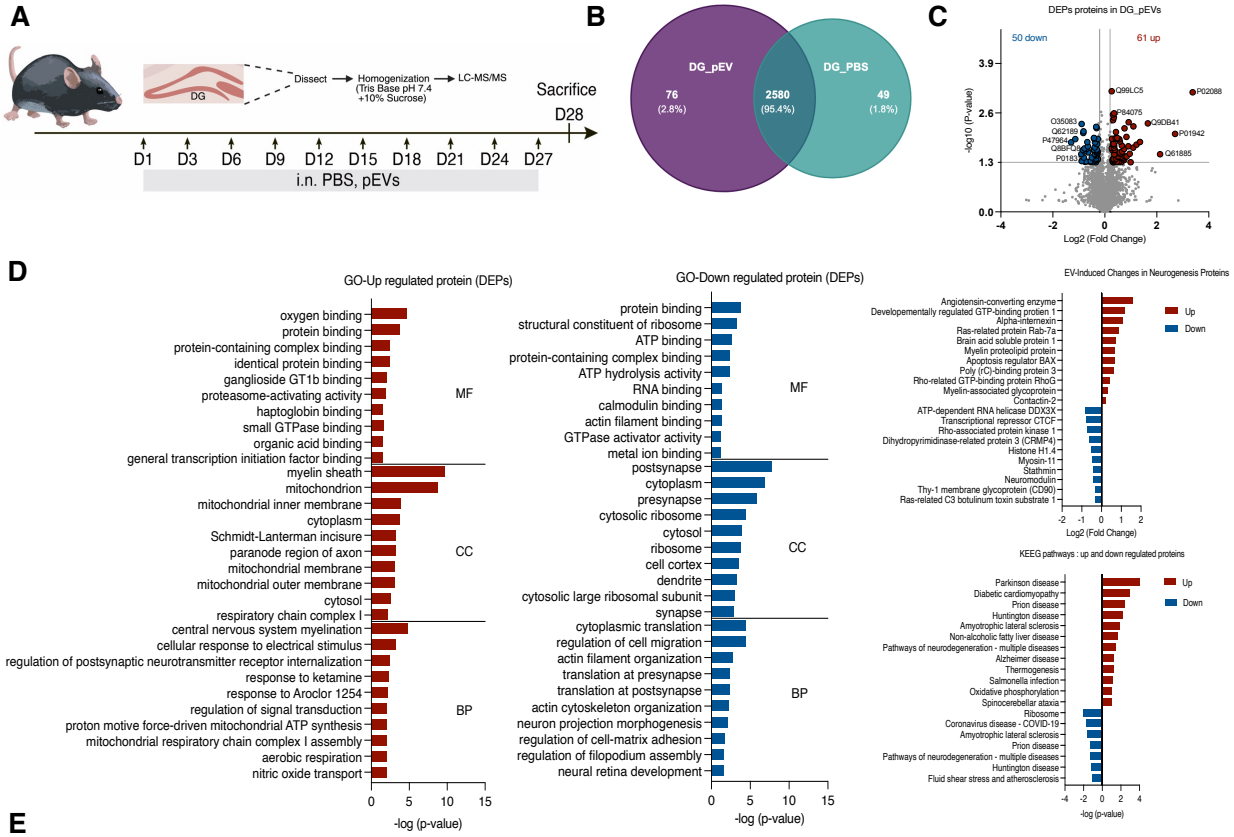
A
DG
Dissect
Homogenization (Tris Base pH 7.4 +10% Sucrose)
LC-MS/MS
Sacrifice
D28
D1 D3 D6 D9 D12 D15 D18 D21 D24 D27
i.n. PBS, pEVs
B
DG_pEV
DG_PBS
76 (2.8%)
2580 (95.4%)
49 (1.8%)
C
DEPs proteins in DG_pEVs
50 down
61 up
-log10 (P-value)
Log2 (Fold Change)
D
GO-Up regulated protein (DEPs)
oxygen binding
protein binding
protein-containing complex binding
identical protein binding
ganglioside GT1b binding
proteasome-activating activity
haptoglobin binding
small GTPase binding
organic acid binding
general transcription initiation factor binding
myelin sheath
mitochondrion
mitochondrial inner membrane
cytoplasm
Schmidt-Lanterman incisure
paranode region of axon
mitochondrial membrane
mitochondrial outer membrane
cytosol
respiratory chain complex I
central nervous system myelination
cellular response to electrical stimulus
regulation of postsynaptic neurotransmitter receptor internalization
response to ketamine
response to Aroclor 1254
regulation of signal transduction
proton motive force-driven mitochondrial ATP synthesis
mitochondrial respiratory chain complex I assembly
aerobic respiration
nitric oxide transport
MF
CC
BP
-log (p-value)
GO-Down regulated protein (DEPs)
protein binding
structural constituent of ribosome
ATP binding
protein-containing complex binding
ATP hydrolysis activity
RNA binding
calmodulin binding
actin filament binding
GTPase activator activity
metal ion binding
postsynapse
cytoplasm
presynapse
cytosolic ribosome
cytosol
ribosome
cell cortex
dendrite
cytosolic large ribosomal subunit
synapse
cytoplasmic translation
regulation of cell migration
actin filament organization
translation at presynapse
translation at postsynapse
actin cytoskeleton organization
neuron projection morphogenesis
regulation of cell-matrix adhesion
regulation of filopodium assembly
neural retina development
MF
CC
BP
-log (p-value)
EV-Induced Changes in Neurogenesis Proteins
Up
Down
Log2 (Fold Change)
KEEG pathways : up and down regulated proteins
Parkinson disease
Diabetic cardiomyopathy
Prion disease
Huntington disease
Amyotrophic lateral sclerosis
Non-alcoholic fatty liver disease
Pathways of neurodegeneration - multiple diseases
Alzheimer disease
Thermogenesis
Salmonella infection
Oxidative phosphorylation
Spinocerebellar ataxia
Ribosome
Coronavirus disease - COVID-19
Amyotrophic lateral sclerosis
Prion disease
Pathways of neurodegeneration - multiple diseases
Huntington disease
Fluid shear stress and atherosclerosis
-log (p-value)
E
-log (p-value)
Threshold
Ribosomal Quality Control Signaling Pathway
SirtuinSignaling Pathway
Nonsense-Mediated Decay (NMD)
Signaling by NOTCH4
Selenoamino acid metabolism
Response of EIF2AK4 (GCN2) to amino acid deficiency
Mitochondrial Dysfunction
Major pathway of rRNA processing in the nucleolus and cytosol
Eukaryotic Translation Elongation
Eukaryotic Translation Termination
Granzyme A Signaling
SRP-dependent cotranslational protein targeting to membrane
Eukaryotic Translation Initiation
Respiratory electron transport
Transport of inorganic cations / anions & amino acids / oligopeptides
Oxidative Phosphorylation
Protein Ubiquitination Pathway
Class I MHC mediated antigen processing & presentation
Neutrophil Extracellular Trap Signaling Pathway
Signaling by Rho Family GTPases
Processing of Capped Intron-Containing Pre-mRNA
Myelination Signaling Pathway
Analysis: DG_EV
positive z-score
z-score = 0
negative z-score
no activity pattern available
ratio
Ratio